Porous Nitrogen-Doped Carbon Derived from Peanut Shell as Anode Material for Lithium Ion Battery

Lian Liu, Lan Yang, Ping Wang, Cao-Yu Wang, Jian Cheng, Geng Zhang[*],
Jiang-Jiang Gu[*] *and Fei-Fei Cao*

College of Science, Huazhong Agricultural University, Wuhan, 430070, People's Republic of China
[*]E-mail: zhanggeng@mail.hzau.edu.cn, jiangjianggu@mail.hzau.edu.cn

The development of anode materials originating from renewable resources with high performance and low cost has become an important research direction in the development of lithium ion batteries (LIBs). Herein, peanut shell, a common biomass, was used as a raw material to synthesize nitrogen-doped carbon applied in the anode of LIBs. The effects of calcination temperature and acid treatment on the electrochemical performance of the peanut shell-derived carbon material were first studied; it was found that a higher calcination temperature will improve the performance of the carbon material. The carbon prepared at 700°C presented a capacity at 180 mA h g^{-1} (0.1 C), much higher than for samples prepared at 300 and 500°C. The acid treatment can further improve the capacity to 320 mA h g^{-1}. On this basis, nitrogen doping was introduced into the carbon material with melamine as the nitrogen source. It was found that the doping method will affect the final properties of the carbon; the nitrogen-doped carbon prepared by a one-pot method (doping and carbonization simultaneously) exhibited a capacity at 570 mA h g^{-1} with quite stable cycling performance, larger than that prepared by a successive method (carbonization followed by doping). This work demonstrates a promising pathway for the utilization of biomass to prepare active anode material for LIBs.

1. INTRODUCTION

Due to the energy shortage and environment pollution caused by traditional fossil fuels, the development of new energy and the use of secondary energy have become hot issues worldwide. As electrochemical energy storage device, lithium ion batteries (LIB) have received considerable attention and have been widely applied in many fields, such as portable devices and electric vehicles, owing to their high capacity, high energy density and long life cycles.[1, 2]

As the active material of lithium storage, the anode material, where lithium insertion and extraction occur during charging/discharging, determines the electrochemical performance of LIB. Carbon-based materials have always been the most commonly used anode materials since the commercialization of LIBs. Carbon-based anode materials have several advantages: (1) the theoretical capacity of graphite is 372 mA h g^{-1}, which is suitable for many portable devices used in daily life; (2) the good electrochemical properties of carbon materials lead to a stable charging/discharging plateau and favorable reversibility; (3) carbon-based anode materials can be produced at a large scale with low cost; (4) the insertion/extraction mechanism of lithium ion in carbon materials and various reactions occurring in the carbon material during charging/discharging have been well studied.[3-6] However, currently used carbon anode materials are predominantly derived from non-renewable resources (*e.g.*, natural gas), which is adverse to the long-term development of LIBs. Therefore, the development of carbon material originating from renewable resources with high performance and low cost has become an important research direction.[7, 8]

Biomass is produced in large amounts every year, but most cannot be utilized properly.[7] Biomass usually contains carbonaceous polymers such as cellulose, hemicellulose and lignin, and thus, all-carbon or partial-carbon materials can be obtained through pyrolysis.[8, 9] In addition to organic components, there are usually inorganic components (*e.g.*, SiO_2 and minerals) present in biomass that can be adopted as pore formers in the final carbon material after removal.[7] As the raw material, biomass is abundant, renewable and low-cost, which is important for its practical application. Therefore, biomass-derived carbon materials are suitable for use as an anode material in LIBs. Many types of biomass, such as bamboo, walnuts, corn stalks, and cotton starch, have been employed to prepare anode carbon material with outstanding performance, which makes biomass a promising resource for the preparation of carbon material in LIBs.[4, 7-10]

Figure 1. Schematic illustration for synthesis of N-doped carbon materials derived from peanut shells.

In this work, we selected peanut shells, which are a common biomass with low cost, as the raw material to prepare porous carbon material for LIB anodes. Although the peanut shell-derived carbonaceous electrode materials have been applied to LIBs,[11-13] these materials usually lack heteroatom doping because the peanut shell is composed of cellulose, hemicellulose and lignin, which

have low levels of heteroatoms. It is well known that heteroatom doping is helpful to improve the electrochemical performance of carbon materials in LIBs.[8, 14] Here, we developed a nitrogen-doped porous carbon material using peanut shells as the precursor with melamine as the nitrogen source (as illustrated in Figure 1). The study results showed that a one-pot nitrogen doping strategy (doping and carbonization simultaneously) accompanied with higher calcination temperature and acid treatment was beneficial to improve the electrochemical performance of the peanut shell-derived carbon material.

2. EXPERIMENTAL SECTION

2.1 Synthesis of carbon materials

Peanut shells were obtained by removing fruits inside the peanut. Firstly, peanut shells were crushed into powder by a tiny plant crusher followed by drying at 80°C for 24 h. Then the peanut shell powder was transferred to a crucible and heated at 300°C, 500°C and 700°C for 3 h in air, respectively. The obtained sample was denoted as C-300, C-500 and C-700, respectively. After immersing in 100 ml HCl solution (2 mol/L) for 24 h, the sample was collected by filtration followed by washing with DI water and drying at 80 °C for 24 h. The finally obtained powder was denoted as C-300-H, C-500-H, and C-700-H, respectively.

To prepare a nitrogen-doped carbon material, the peanut shell powder and melamine (3:1 by weight) were mixed and thoroughly ground in a mortar for 15 min. Subsequently, the mixture was placed in a crucible and heated at 700°C for 3 h in air. After cooling naturally, the sample was immersed in 100 ml HCl (2 mol/L) for 24 h, followed by filtration, washing with DI water and drying at 80°C for 24 h. The powder finally obtained was denoted NC-700-I. In comparison, the peanut shell powder was replaced by C-700-H, which was mixed with melamine (3:1 by weight) followed by heating in a tube furnace under Ar at 700°C for 3 h. The obtained sample was named NC-700-II.

2.2 Characterizations

The crystalline structure of the sample was characterized using an X-ray diffractometer (XRD, JDX-10P3A) with a filtered Cu Kα radiation source. Raman spectra were recorded on a Renishaw1000 spectrometer with the 514.5-nm line of Ar-ion laser as excitation source. The X-ray photoelectron spectroscopy (XPS) of the sample was recorded on an ESCALab 250Xi spectrometer (Thermo Scientific). The morphology of the material was observed using a scanning electron microscope (SEM, JSM-6390LV).

2.3 Electrochemical measurements

Electrochemical measurements were performed on coin-type CR 2032 cells assembled in an argon-filled glovebox (Mikrouna, Super (1220/750)). The working electrode was fabricated by

depositing the mixed slurry of active material, Super P and PVDF binder in N-methyl-2-pyrrolidone (NMP) solvent with a weight ratio of 8:1:1 onto Cu foil and drying at 80°C in a vacuum oven for 12 h. Lithium foil was used as the counter electrode and a glass fiber (GF/D) membrane (Whatman) was used as the separator. The electrolyte was 1 M $LiPF_6$ dissolved in a mixed solvent of ethylene carbonate (EC), dimethyl carbonate (DMC) and diethyl carbonate (volume ratio 1:1:1). The charging/discharging tests were performed between 0.01-3 V with a Land CT2001 battery tester (Wuhan Land Electronic Co. Ltd., China).

3. RESULTS AND DISCUSSION

3.1 Material Characterizations

The crystalline structure of the product was studied using XRD. As shown in Figure 2a, there are two broad peaks at approximately 23° and 43° for all four curves, which can be indexed to the (002) and (100) plane of carbon materials, respectively. It is well accepted that the (002) peak indicates the parallel stacking degree of the graphene sheets, while the (100) peak comes from the sp^2-hybridized carbon, which is a descriptor to the lateral extent of the graphene sheets.[15-17] With an increase in calcination temperature from 300°C to 700°C, the (100) peak become more and more prominent and narrow, indicating the improvement of the graphitization degree from C-300 to C-700. The empirical *R* factor, defined as the (002) peak-to-background ratio (shown in Figure 2b), reflects the proportion of graphene layers stacking in a parallel architecture.[15, 17, 18] Here, the *R* factor for C-700 is 1.64, which is lower than for materials reported previously,[15, 17, 18] indicating that C-700 has more non-parallel single graphene sheets, which benefit the lithium insertion capacity[15, 18]. The XRD pattern of the acid-treated sample (C-700-H) is also shown in Figure 2a. The *R* factor of C-700-H is 2.17, which is higher than that of C-700, indicating that the degree of parallel stacking of graphene sheets improved; this improvement may be caused by the removal of impurities and ash from the sample by acid treatment. Although the higher *R* factor is adverse to the insertion of lithium, the conductivity and average micropore size of the material will be improved,[17] benefitting application of carbon material in LIBs.

Due to the high graphitization degree, we chose 700°C as the preparation temperature to synthesize a nitrogen-doped sample (NC-700-I) by calcination of the mixture of peanut shells and melamine. Figure 2c shows the XPS full survey of NC-700-I, where three elements, C, N and O, can be detected. The nitrogen content of NC-700-I was 2.6%, while that of un-doped C-700-H was nearly zero. The high-resolution N 1s XPS spectrum of NC-700-I (Figure 2d) presents four N species: pyridinic N (398.4 eV), pyrrolic N (400.1 eV), graphitic N (401.1 eV) and oxidized N (403.8 eV), which indicates that nitrogen is successfully doped into the carbon lattice. [19] Raman spectroscopy is a technique with higher sensitivity for structural changes of carbon than XRD, where the D-band represents the defects and disordered portions of carbon, the G-band indicates the ordered graphitic degree of carbon, and the I_D/I_G value (*i.e.*, intensity ratio between D band and G band) is usually used to assess the amount of defects in carbon materials.[20] As shown in Figure 2e, the I_D/I_G ratio for C-

700-H and NC-700-I is 1.01 and 1.00, respectively, higher than many biomass-derived carbon materials,[15, 16, 18, 21, 22] indicating the presence of large numbers of defects or disordered carbon in both C-700-H and NC-700-I, which can provide more active sites to facilitate the diffusion of Li ions.[23]
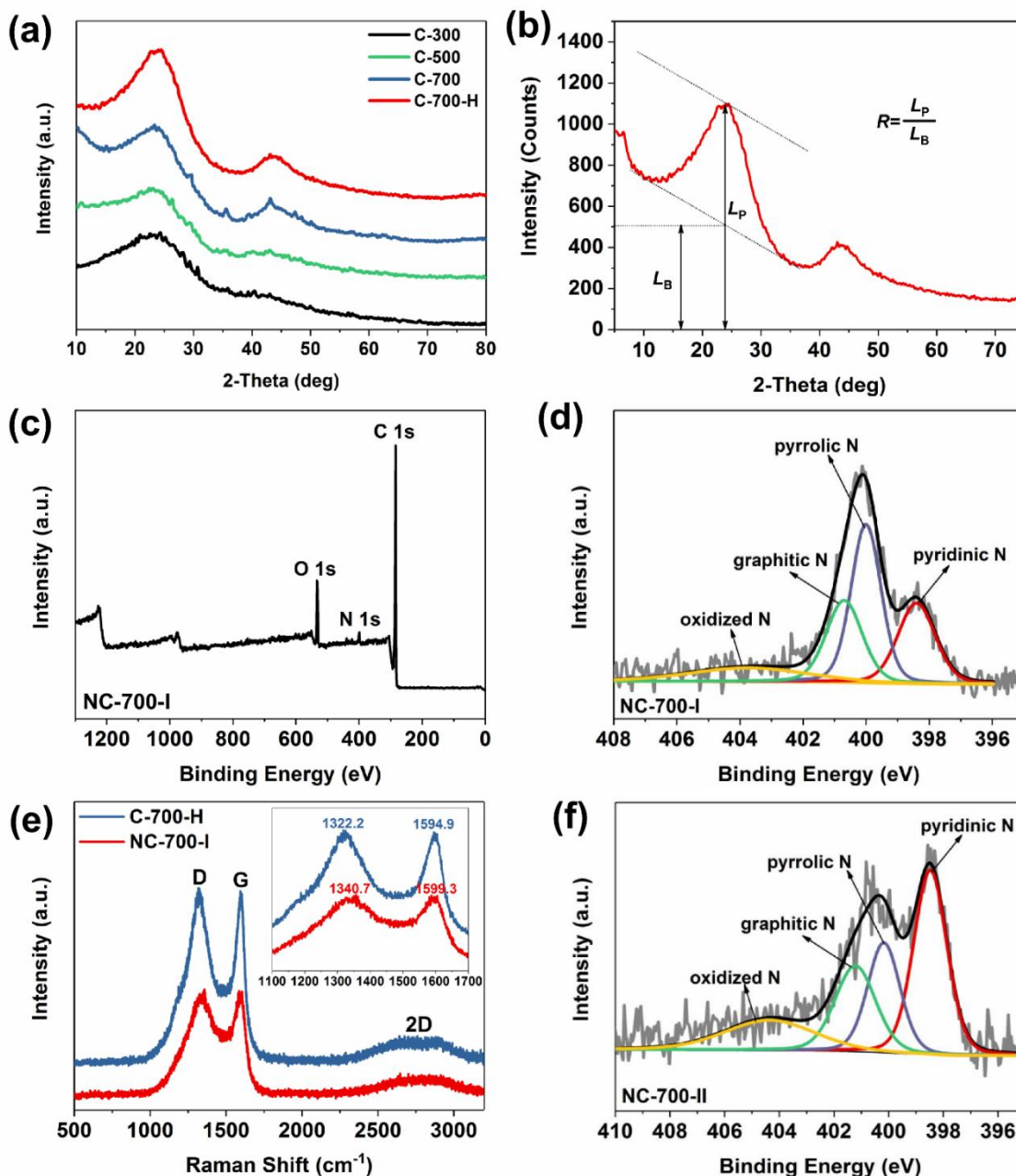
Figure 2. (a) XRD patterns of C-300, C-500, C-700, and C-700-H. (b) Illustration of definition of *R* factor of (002) peak. (c) XPS full survey spectra of NC-700-I. (d) High-resolution N 1s XPS spectrum of NC-700-I. (e) Raman spectra of C-700-H and NC-700-I; inset shows partial enlarged view of spectra. (f) High-resolution N 1s XPS spectrum of NC-700-II.

In addition, the inset of Figure 2e shows that the D and G bands of NC-700-I are shifted positively compared to C-700-H due to structural distortion, which also supports the doping of

nitrogen in the lattice of graphite.[24] Nitrogen doping will give rise to higher conductivity and more active sites in NC-700-I, which benefits its electrochemical performances in LIBs.[25-28]
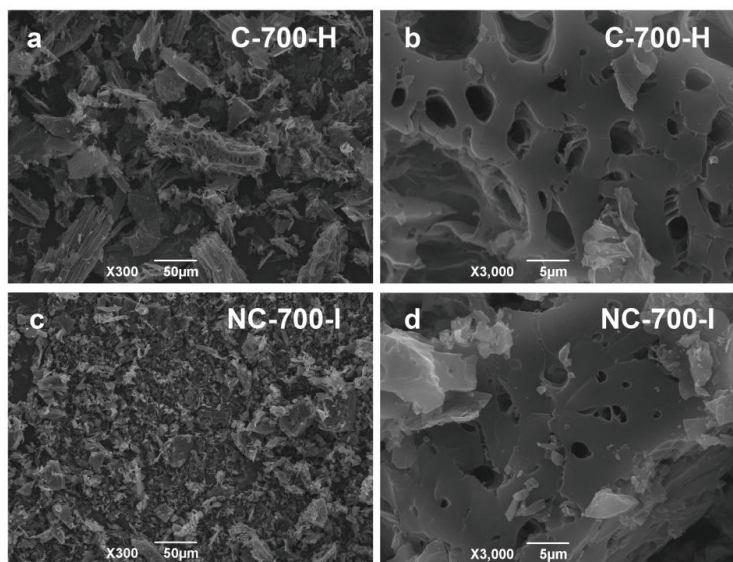
Figure 3. SEM images of (a, b) C-700-H and (c, d) NC-700-I.

The SEM image in Figure 3a shows that C-700-H is composed of micro-sized carbon particles. A more highly magnified image (Figure 3b) proves the presence of macropores and cavities in C-700-H with a pore size from several to approximately 10 microns, similar to the result reported by Cao et al.[13] The porous structure of C-700-H is beneficial for the insertion and extraction of lithium ions. The SEM images of NC-700-I, a nitrogen-doped material, are shown in Figure 3c and 3d. Figure 3c shows that the particle size of NC-700-I is smaller than for C-700-H. Figure 3d demonstrates that NC-700-I possesses a porous structure as well, *i.e.*, nitrogen doping during calcination does not disturb the formation of pores in the carbon material. Notably, the macropore size of NC-700-I almost distributes below 5 μm (Figure 3d), smaller than for C-700-H. The decreases in particle size and pore size will improve the surface area of the carbon material, which will subsequently enhance the electrochemical performance of NC-700-I.[16]

3.2 Electrochemical performances

Table 1. Charge capacity, discharge capacity and columbic efficiency for various materials at first charging/discharging cycle (0.1 C).

	Initial discharge capacity mA h g^{-1}	Initial charge capacity mA h g^{-1}	Initial columbic efficiency %
C-300	181.6	15.6	8.6
C-500	254.7	17.8	7
C-700	684.6	195.7	28.6
C-700-H	971.3	225.7	23.2
NC-700-I	917.5	369.8	40.3
NC-700-II	801.7	266.7	33.3

As listed in Table 1, the initial discharge/charge capacity (0.1 C) of C-300 and C-500 is 181.6/15.6 and 254.7/17.8 mA h g^{-1}, respectively. Correspondingly, the initial columbic efficiency of C-300 and C-500 is only 8.6% and 7%, respectively, indicating a large irreversible capacity. In sharp contrast, the initial charge/discharge capacity of C-700 can reach up to 684.6/195.7 mA h g^{-1}, and thus the initial columbic efficiency is increased to 28.6%. The low columbic efficiency in the first discharge/charge cycle is common for carbonaceous anode materials, which may be attributed to the following reasons: 1) formation of solid electrolyte interphase (SEI) films on the surface of carbon caused by the decomposition of carbonate-based electrolyte; 2) irreversible Li insertion due to highly disordered carbon structure with hydroxyls and/or adsorbed water on the surface of the carbon material. [15, 21, 22, 29] Herein, C-700 possessed a much higher initial columbic efficiency than C-300 and C-500, indicating that the stability and degree of structural ordering of carbon material were obviously improved with calcination temperature. In the subsequent discharge/charge cycles (Figure 4), the specific capacity of C-700 at 0.1 C fluctuated near 225 mA h g^{-1}, which is significantly higher than that of C-300 (19 mA h g^{-1}) and C-500 (7 mA h g^{-1}). This large improvement in specific capacity can be observed at other rates (Figure 4): the specific capacity of C-700 under 0.2 C, 0.5 C, 1 C, 2 C, 5 C can reach 193, 160.9, 123.4, 86.8 and 23.8 mA h g^{-1}, respectively; in contrast, the specific capacity of samples C-300 and C-500 at higher rates (>0.2 C) was almost zero. Additionally, the columbic efficiency during the entire period of rate performance testing was near 100%, indicating high stability against discharge/charge cycling (Figure 4). These results demonstrated that high calcination temperature can significantly improve the electrochemical capability of the peanut shell-derived carbon material, which may be due to enhanced conductivity as reflected by higher graphitization degree (Figure 2a) and improved initial columbic efficiency.
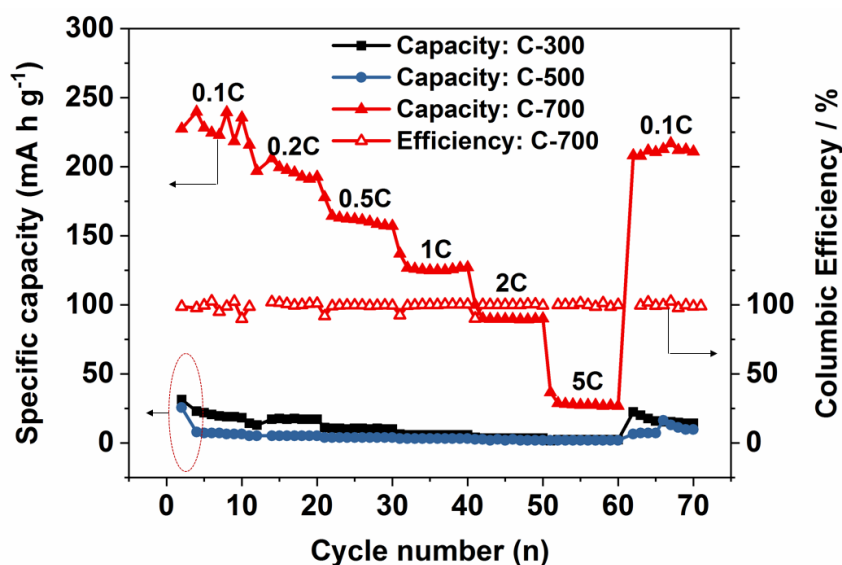
Figure 4. Rate capability for C-300, C-500 and C-700 and columbic efficiency of C-700.

The effect of acid treatment on the electrochemical performance of peanut shell-derived carbon material was studied. Figure 5a and 5b display the comparison of C-700 and C-700-H in terms of initial charge/discharge test and rate capability. After acid treatment, C-700-H presents an enhanced

first discharge and charge capacity up to 917.3 and 225.7 mA h g^{-1}, respectively (Table 1), which indicated that acid treatment can improve the lithium storage capacity of this carbon material. Moreover, the specific capacity of C-700-H is higher than C-700 under 0.1 C, 0.2 C and 0.5 C, with a columbic efficiency near 100% (Figure 5b).
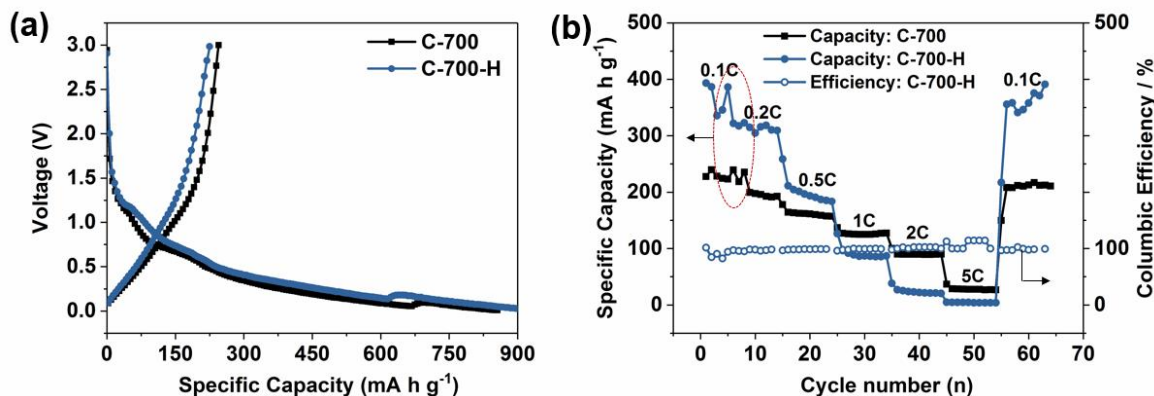
Figure 5 (a) First charge/discharge curves of C-700 and C-700-H at rate of 0.1 C and (b) rate capability of C-700 and C-700-H together with columbic efficiency of C-700-H.

It is well known that various inorganic minerals in biomass materials cannot be removed by pyrolysis and carbonization.[7] However, acid treatment can effectively remove these components and thus enhance the porosity of the carbon material, which provides a fast transmission channel for the transport of electrolytes, thereby increasing the capacity of C-700-H. This speculation can be supported by the fact that the *R* factor of C-700-H (2.17) is higher than for C-700 (1.64). Dahn et al. [17] have shown that the increased *R* factor was accompanied by an increased average micropore size of the carbon material.
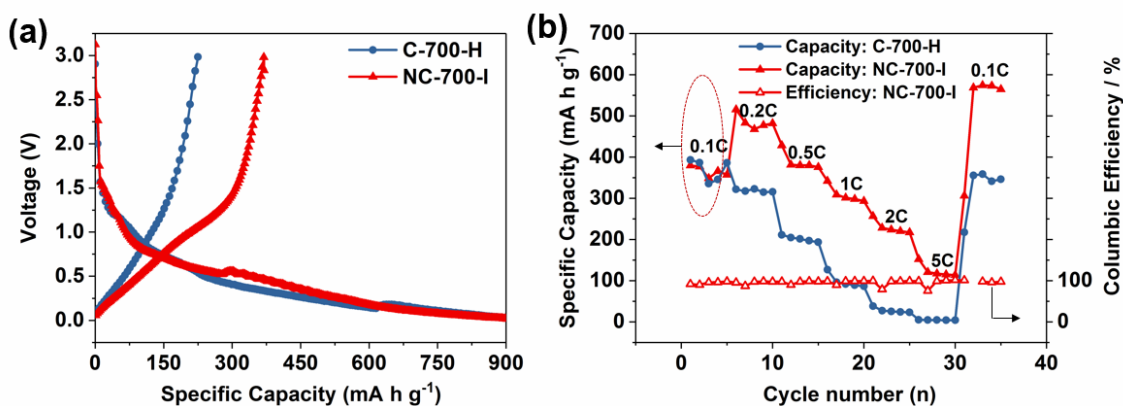
Figure 6 (a) First charge/discharge curves of C-700-H and NC-700-I at rate of 0.1 C and (b) rate capability of C-700-H and NC-700-I with columbic efficiency of NC-700-I.

Heteroatom-doping (*e.g.*, N, B and S) has been reported to be another effective method to improve the electrochemical performance of carbonaceous anode materials due to enhanced conductivity and lithium storage capacity.[6, 14, 24, 26-28] Figure 6a shows that the nitrogen-doped

carbon material (NC-700-I) exhibits an initial discharge/charge capacity at 917.5/369.8 mA h g^{-1} with a columbic efficiency at 40.9%, much higher than that of nitrogen-free C-700-H (Table 1). Compared to C-700-H, the specific capacity of NC-700-I under 0.1 C, 0.2 C, 0.5 C, 1 C, 2 C and 5 C increased by 30, 144, 177, 219 and 116 mA h g^{-1}, respectively (Figure 6b), illustrating that nitrogen doping can efficiently enhance the electrochemical performance of carbon materials. It is widely accepted that nitrogen doping sites can attract more Li ions due to the higher electronegativity of nitrogen atoms. Moreover, the modification of electronic properties of the carbon matrix and introduction of topological defects in the material via nitrogen doping are also beneficial to increase the storage capacity of Li ions.[26-28] In addition, the specific capacity of NC-700-I after high current density cycling was recovered to 570 mA h g^{-1}, even higher than the pristine value. Moreover, the columbic efficiency of NC-700-I was always near 100% from 0.1 C to 5 C (Figure 6b), demonstrating quite stable cycling performance. As tabulated in Table 2, the specific capacity of the NC-700-I anode material was better than or comparable to recently reported biomass-derived carbon anodes for LIBs, likely due to nitrogen doping and the special structure of NC-700-I.
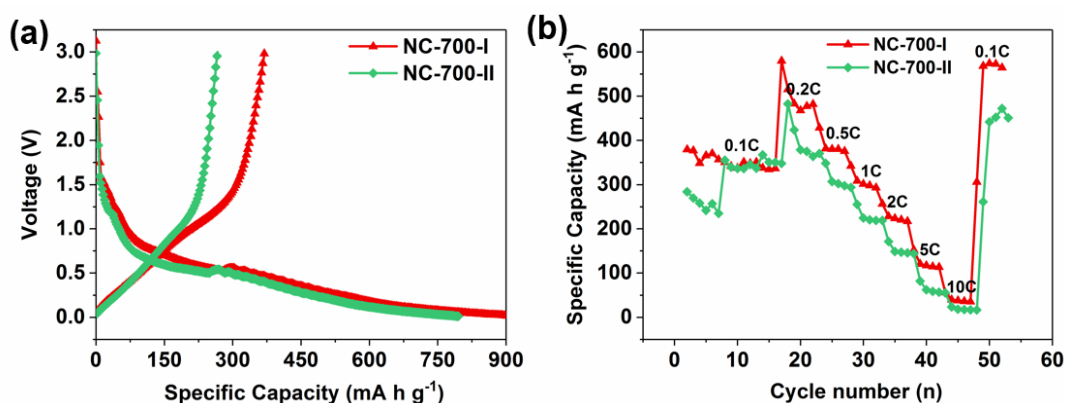
Figure 7. (a) First charge/discharge curves of NC-700-I and NC-700-II at rate of 0.1 C and (b) rate capability of NC-700-I and NC-700-II.

Table 2. Comparison of specific capacity between NC-700-I and other recently reported biomass-derived anode materials in LIBs.

Anode Material	Raw Material	Specific Capacity / mA h g^{-1}				Reference
		0.1 C	0.2 C	1 C	2 C	
NC-700-I	Peanut shell	350(570)[a]	480	300	225	This Work
W-900	Microalgae	445	n.a.	370	n.a.	[16]
1100CSTs	Mushroom	n.a.	289	n.a.	n.a.	[30]
Carbon nanoparticles/ graphene composites	Sodium alginate	n.a.	n.a.	n.a.	268.1	[21]
C-100-750	Sodium alginate	n.a.	n.a.	263.9	222.8	[22]
activated carbon	Sisal	~250	n.a.	n.a.	n.a.	[15]
RH-Acid-HTC-900-HF	Rice husk	n.a.	n.a.	199	164	[29]

[a] 570 mA h g^{-1} is obtained when the rate was returned to 0.1 C.

Nitrogen doping methods were also explored. In addition to the one-pot method (doping and carbonization simultaneously) mentioned above, a successive method (carbonization followed by doping) was tested, wherein melamine was treated with the as-prepared carbon material (C-700-H) at 700°C and gave rise to NC-700-II. The successful doping of nitrogen in NC-700-II was confirmed by XPS (Figure 2f), where four N species were observed. The initial charge/discharge capacity of NC-700-II is 266.7 and 801.7 mA h g^{-1}, respectively, and thus the initial columbic efficiency is 33.3% (Figure 7a and Table 1), all of which are lower than those of NC-700-I. In addition, the specific capacity of NC-700-I is always higher than that of NC-700-II under different rates (Figure 7b). Hence, we can conclude that the product synthesized by the one-pot method produces a better electrochemical performance than that of material produced by post nitrogen doping. It is believed that the nitrogen atom can more easily insert into the lattice of carbon material during the carbonization of peanut shells. If the carbon has been formed, it is more difficult for the nitrogen atom to dope into the carbon lattice, thereby explaining why NC-700-I has a higher nitrogen content (2.6% from XPS) than NC-700-II (2.2%).

4. CONCLUSIONS

In this work, we explored a simple method to synthesize the anode material of LIB using peanut shells as the carbon source. Studies have shown that a higher calcination temperature and acid treatment can improve the electrochemical performances of peanut shell-derived carbon materials. On this basis, nitrogen doping can increase performance, but the doping method will affect the final properties of the carbon: nitrogen-doped carbon prepared by one-pot method (doping and carbonization simultaneously) exhibited a greater capacity larger than carbon prepared using a successive method (carbonization followed by doping). This work demonstrated a promising pathway for the utilization of biomass to prepare active anode materials of LIBs.

References

1. W.D. Li, B.H. Song and A. Manthiram, *Chem. Soc. Rev.*, 46 (2017) 3006.
2. F.X. Wu and G. Yushin, *Energy Environ. Sci.*, 10 (2017) 435.
3. N. Mahmood, T.Y. Tang and Y.L. Hou, *Adv. Energy Mater.*, 6 (2016) DOI: 10.1002/aenm.201600374.
4. Y. Yao and F. Wu, *Nano Energy*, 17 (2015) 91.
5. D.S. Su and R. Schlogl, *ChemSusChem*, 3 (2010) 136.
6. L.G. Bulusheva, A.V. Okotrub, A.G. Kurenya, H. Zhang, H. Zhang, X. Chen and H. Song, *Carbon*, 49 (2011) 4013.
7. L. Zhang, Z. Liu, G. Cui and L. Chen, *Prog. Polym. Sci.*, 43 (2015) 136.

8. W.J. Tang, Y.F. Zhang, Y. Zhong, T. Shen, X.L. Wang, X.H. Xia and J.P. Tu, *Mater. Res. Bull.*, 88 (2017) 234.
9. P. Kalyani and A. Anitha, *Int. J. Hydrogen Energy*, 38 (2013) 4034.
10. R.R. Gaddam, D. Yang, R. Narayan, K.V.S.N. Raju, N.A. Kumar and X.S. Zhao, *Nano Energy*, 26 (2016) 346.
11. W.M. Lv, F.S. Wen, J.Y. Xiang, J. Zhao, L. Li, L.M. Wang, Z.Y. Liu and Y.J. Tian, *Electrochim. Acta*, 176 (2015) 533.
12. J. Ding, H.L. Wang, Z. Li, K. Cui, D. Karpuzov, X.H. Tan, A. Kohandehghan and D. Mitlin, *Energy Environ. Sci.*, 8 (2015) 941.
13. X.Y. Cao, S.Q. Chen and G.X. Wang, *Electron. Mater. Lett.*, 10 (2014) 819.
14. T.J. Bandosz and T.Z. Ren, *Carbon*, 118 (2017) 561.
15. X. Yu, K. Zhang, N. Tian, A. Qin, L. Liao, R. Du and C. Wei, *Mater. Lett.*, 142 (2015) 193.
16. H. Ru, N. Bai, K. Xiang, W. Zhou, H. Chen and X.S. Zhao, *Electrochim. Acta*, 194 (2016) 10.
17. J.R. Dahn, W. Xing and Y. Gao, *Carbon*, 35 (1997) 825.
18. X. Sun, X. Wang, N. Feng, L. Qiao, X. Li and D. He, *J. Anal. Appl. Pyrolysis*, 100 (2013) 181.
19. D.W. Wang and D.S. Su, *Energy Environ. Sci.*, 7 (2014) 576.
20. F. Pan, J. Jin, X. Fu, Q. Liu and J. Zhang, *ACS Appl. Mater. Interfaces*, 5 (2013) 11108.
21. H. Xing, F. Zhang, Y. Lu, B. Zhai, S. Zhai, Q. An and C. Yu, *RSC Adv.*, 6 (2016) 79366.
22. Z. Wang, F. Zhang, Y. Lu, B. Zhai, S. Zhai, Z. Xiao, Q. An, C. Yu and S. Gao, *Mater. Res. Bull.*, 83 (2016) 590.
23. P. Wang, G. Zhang, Z. Li, W. Sheng, Y. Zhang, J. Gu, X. Zheng and F. Cao, *ACS Appl Mater Interfaces*, 8 (2016) 26908.
24. Z.-S. Wu, W. Ren, L. Xu, F. Li and H.-M. Cheng, *ACS Nano*, 5 (2011) 5463.
25. J. Zhang, L. Zhang, S. Yang, D. Li, Z. Xie, B. Wang, Y. Xia and F. Quan, *J. Alloy. Compd.*, 701 (2017) 256.
26. L. Qie, W.-M. Chen, Z.-H. Wang, Q.-G. Shao, X. Li, L.-X. Yuan, X.-L. Hu, W.-X. Zhang and Y.-H. Huang, *Adv. Mater.*, 24 (2012) 2047.
27. W.H. Shin, H.M. Jeong, B.G. Kim, J.K. Kang and J.W. Choi, *Nano Lett.*, 12 (2012) 2283.
28. H. Wang, C. Zhang, Z. Liu, L. Wang, P. Han, H. Xu, K. Zhang, S. Dong, J. Yao and G. Cui, *J. Mater. Chem.*, 21 (2011) 5430.
29. L. Wang, Z. Schnepp and M.M. Titirici, *J. Mater. Chem. A*, 1 (2013) 5269.
30. B. Campbell, R. Ionescu, Z. Favors, C.S. Ozkan and M. Ozkan, *Sci. Rep.*, 5 (2015) 14575.